

Auto-Lesion Segmentation with a Novel Intensity Dark Channel Prior for COVID-19 Detection

Basma Jumaa Saleh^{1,4,*}, Zaid Omar¹, Vikrant Bhateja², Lila Iznita Izhar³

¹ Department of Electronic and Computer Engineering, Faculty of Electrical Engineering, Universiti Teknologi Malaysia, Malaysia

² Department of Electronics Engineering, Veer Bahadur Singh Purvanchal University, India.

³ Department of Electrical and Electronic Engineering, Universiti Teknologi PETRONAS, Malaysia

⁴ Department of Computer Engineering, Mustansiriyah University, Iraq

Email: saleh.b@graduate.utm.my

Abstract. During the COVID-19 pandemic, medical imaging techniques like computed tomography (CT) scans have demonstrated effectiveness in combating the rapid spread of the virus. Therefore, it is crucial to conduct research on computerized models for the detection of COVID-19 using CT imaging. A novel processing method has been developed, utilizing radiomic features, to assist in the CT-based diagnosis of COVID-19. Given the lower specificity of traditional features in distinguishing between different causes of pulmonary diseases, the objective of this study is to develop a CT-based radiomics framework for the differentiation of COVID-19 from other lung diseases. The model is designed to focus on outlining COVID-19 lesions, as traditional features often lack specificity in this aspect. The model categorizes images into three classes: COVID-19, non-COVID-19, or normal. It employs enhancement auto-segmentation principles using intensity dark channel prior (IDCP) and deep neural networks (ALS-IDCP-DNN) within a defined range of analysis thresholds. A publicly available dataset comprising COVID-19, normal, and non-COVID-19 classes was utilized to validate the proposed model's effectiveness. The best performing classification model, Residual Neural Network with 50 layers (Resnet-50), attained an average accuracy, precision, recall, and F1-score of 98.8%, 99%, 98%, and 98% respectively. These results demonstrate the capability of our model to accurately classify COVID-19 images, which could aid radiologists in diagnosing suspected COVID-19 patients. Furthermore, our model's performance surpasses that of more than 10 current state-of-the-art studies conducted on the same dataset.

1. Introduction

The World Health Organization (WHO) declared the COVID-19 virus as a pandemic in 2020 [1]. In addressing this illness, among the most common diagnostic procedures is called reverse transcription polymerase chain reaction (RT-PCR), but it has several potential drawbacks that make it less reliable than other approaches [2]. It has been determined that chest computed tomography (CT) is a useful adjunctive technique for detection COVID-19. Chest CT exhibits high sensitivity in screening for COVID-19 infection and can provide a prompt diagnosis, particularly when compared to the RT-PCR

test [3]. Chest radiography has been helpful for the diagnosis, observation, and monitoring or tracking of COVID-19 progression when its natural history is evaluated [4]. Although chest X-rays are routinely taken, CT scans are far more sensitive than X-rays in detecting diseases. CT scans can effectively identify patchy ground-glass opacities (GGOs) and consolidations [5]. Despite the numerous benefits of lung ultrasound, such as no radiation, lower risk of contamination, reduced cost, and high reproducibility, there are also some drawbacks [6], compared to chest CT scans, it is less sensitive, which is one of its drawbacks [7]. Another limitation of ultrasonography is its limited ability to detect deep and intrapulmonary abnormalities [8]. More commonly, the major drawbacks of magnetic resonance imaging (MRI) that need to be discussed include the small sample size, potential lack of experience leading to restricted repeatability of the suggested protocol, and the necessity to allocate an MRI room to handle the needs of both COVID-19 and non-COVID-19 cases [4].

High-sensitivity computed tomography (CT) scans serve as an alternative option for the early detection of COVID-19, capable of addressing the limitations of PCR. A CT scan can achieve approximately 88% to 98% sensitivity [9]. According to authors [10], [11], RT-PCR's sensitivity in their analysis was inferior to chest CT's (59-71% versus 88-98%, respectively, $P < .001$). Furthermore, evaluation of COVID-19 lung impairment can be done using chest computed tomography (CT) as mentioned in [12], COVID-19 lung damage is typically indicated by numerous and peripheral ground-glass opacities (GGO) and potential concomitant consolidations. In comparison to RT-PCR in symptomatic patients, also found that chest CT had high sensitivity (97%) but intermediate specificity (56%) in patients.

Furthermore, in clinical practice, CT scans have limited specificity (approximately 34%) in detecting COVID-19 and differentiating it from other types of pneumonia based on traditional features [9]. To enhance early diagnosis, the development of novel approaches in medical imaging, such as texture radiomics analysis and mathematical strategies for extracting important features from images across different grayscales, appears crucial [13]. The sub-visual extraction of radiomic properties allows the computer to identify structures that may be imperceptible to the human eye. As a result, radiomics has the potential to complement traditional radiological evaluation by providing valuable clinical data [14].

On the other hand, numerous studies have attempted to merge the two concepts and focus on distinguishing between pneumonia infection and COVID-19 infection, which can pose a challenging task for researchers. The high similarity in CT-traditional findings, attributed to the absence of significant results [15]–[18], makes this differentiation difficult. However, this study solely focuses on distinguishing between COVID-19 and normal cases, achieving high accuracy [19]. Furthermore, studies [20] and [21] have focused on segmenting regions of interest to extract radiomics features and achieve optimal results in multi-class classification. Many of these studies involve the manual segmentation of the entire volume of interest (VOI) for pneumonia lesions within the lungs, utilizing a popular open-source software package [21].

To enable a rapid, consistent, and human error immune framework for pulmonary and lung assessment, an artificially intelligent system has been utilized to semi-automatically segment pneumonia lesions in various studies. In this current work, a new radiomics feature technique called Auto-lesion segmentation (ALS) is suggested for the diagnosis of COVID-19 using computed tomography imaging. The ALS technique utilizes an intensity dark channel prior based on a Deep Neural Network (ALS-IDCP-DNN) model. The suggested methodology comprises three primary steps: data resizing, feature extraction and selection, segmentation, data augmentation, and classification. Diseased lung areas are upsampled during the pre-processing stage, and the dataset is augmented using doubling and resizing techniques. During the radiomics feature extraction step, the intensity features are extracted, selected, and the dataset is automatically segmented using the dark channel prior technique. As for the outcome, the classification task was performed using the DNN-based Resnet-50 architecture.

The experimental research utilized a COVID-CT dataset comprising COVID-19, normal, and non-COVID-19 virus types. The test results demonstrated a 98.8% success rate in accurately identifying COVID-19 infections. These results demonstrate that the proposed ALS-IDCP-DNN model performs exceptionally well in identifying the COVID-19 virus. In this research, the ALS-IDCP-DNN model

presents several key contributions to COVID-19 diagnosis using CT scans. Firstly, a framework for classifying COVID-19 was developed, utilizing methods for auto-segmentation, feature extraction, feature selection, and detection. Secondly, a novel radiomics feature extraction method was proposed, which combines IDCP and Guided specific threshold range techniques to enhance analysis and selection. The proposed framework demonstrated high accuracy in classifying CT images as either COVID-19 or non-COVID-19/healthy using only 996 chest CT scan samples, a small number of parameters, and minimal processing resources. The model was tested using three datasets (images of COVID-19 CT scans, non-COVID-19 CT scans, and healthy CT scans images) and outperformed prior works in terms of both explainable detection and precise COVID-19 case classification.

2. Methodology

In this work, a new model is proposed for detecting COVID-19 lesions. The proposed approach involves classifying images into three categories (COVID-19, non-COVID-19, or normal) by exploring the enhancement and automatic segmentation principles of intensity regions of interest (IROIs) based on the dark channel prior (DCP). During the segmentation stage, the areas of interest were found automatically inside the pulmonary lesions. For each lesion, the intensity of the radiomic feature was delineated using a specific range of analysis thresholds. Subsequently, the deep neural network model based on the augmentation process, namely the ALS-IDCP-DNN model, was applied. This study attempts to reduce the number of misdiagnoses caused by human error when interpreting chest CT scans. Its secondary purpose is to facilitate the rapid identification of patients with confirmed COVID-19 infection, other pneumonia diseases, and healthy individuals for the benefit of medical professionals. The proposed ALS-IDCP-DNN model consists of six main points, as follows:

1. Input a real-world dataset collected from CT scans that is available to the public.
2. Images from CT scans are resized to better highlight any regions that might be affected by COVID-19 and preserve homogeneity in features.
3. Extraction and analysis of the radiomic intensity features using the dark channel prior approach for infected lesions.
4. Auto-segmentation by enhancing the brightness of pixels within the specified threshold range of analysis.
5. Double data augmentation is employed to expand the dataset size during the process of resizing imagery.
6. The previously trained ResNet-50 model is utilized to extract deep features from each image. The classification outcomes are then determined based on the categorization of these deep features obtained from each deep structure.
7. The theoretical foundation and dataset utilized by the suggested ALS-IDCP-DNN model are described below.

2.1. Data Sources and Analysis

In this paper, the actual dataset of COVID-19 CT scan digital images used in this project was created by Yang et al. [22], The dataset contains clinical information for 216 COVID-19 patients and 91 non-COVID-19 patients. This dataset includes 349 positive COVID-19 cases and 463 negative Chest Computed Tomography images for lung diseases (with lesions)/health (no lesions). The positive and negative images were gathered from bioRxiv1 (<https://www.biorxiv.org>) and medRxiv2 (<https://www.medrxiv.org>). This dataset has been obtained and developed by an authoritative study on COVID-19 CT patient cases and has been made available to the public.

The CT images are available in a variety of sizes equivalent to height (max = 1853, average = 491, and min = 153) and width (max = 1485, average = 383, and min = 124). Based on the available data, the average age of the unhealthy patients is estimated to be around 45 years old, with 86 males outnumbering 51 females. The usefulness of this dataset has been verified in accordance with standard practices in radiology.

2.2. Proposed Scenarios

The main objective of this proposed effort is to increase the speed at which radiomics analysis can be conducted. This was achieved by having a radiologist with 10 years of experience in lung CT imaging manually identify the region of interest (ROI) within a lesion on a single CT image slice. This was achieved by having a radiologist with 10 years of experience in lung CT imaging manually identify the region of interest (ROI) within a lesion on a single CT image slice. When multiple lesions were present, the one with the largest volume and/or highest density was chosen as the target for the region of interest (ROI). In this section, the problem of auto-segmentation of the ROI on the chest CT medical image, extracting the radiomics feature of this region, and selecting the necessary features is presented using a modified dark channel prior (DCP).

The dark channel prior can directly estimate the thickness of haze in an image by analysing pixels with low intensity. In addition, the lung lesion tissue shares similarities with haze in an image. Based on the above, an automatic segmentation scheme was applied to the lungs and extracted using a modified DCP. The purpose was to estimate the threshold of the included intensity for increasing pixel brightness, specifically targeting the removal of haze (representing lung lesion tissue) from the pixels. Subsequently, the intensity was carefully observed in the analysis of most images to best distinguish COVID-19 lesions from other pulmonary conditions within a specific threshold range. This approach outperformed current state-of-the-art techniques and required minimal processing time. The process is outlined as follows:

2.2.1. Dark Channel Prior (DCP)

The dark channel prior technique largely relies on the characteristics of haze-free images. In general, pixels with very low intensity, virtually zero in at least one colour channel, can be found in areas that are not covered by the sky, with details mentioned by [23]. To clearly describe this finding, researchers must first specify the mean of "dark channel." If you take any image in \mathfrak{J} and look at its dark channel, The source of $\mathfrak{J}^{\text{DCP}}$ is:

$$\mathfrak{J}^{\text{DCP}}(x) = \text{Min}_{y \in \mathcal{C}(x)} (\text{Min}_{y \in \{r,g,b\}} \mathfrak{J}^c(y)) \quad (1)$$

where \mathfrak{J}^c is a color-channel of \mathfrak{J} and $\mathcal{C}(x)$ is a localized area centred at x . Two minimum operators yielding a dark channel: $\text{Min}_{y \in \{r,g,b\}}$ is achieved on each pixel, and $\text{Min}_{y \in \mathcal{C}(x)}$ is a lower limit filter. Commutativity holds for the operator minimum.

If \mathfrak{J} is a haze free external image other than the sky locale, our analysis indicates that the brightness of \mathfrak{J} 's dark channel is small and is typically zero:

$$\mathfrak{J}^{\text{DCP}} \rightarrow 0 \quad (2)$$

The study in [23] provided a straightforward technique for calculating the globally atmospheric light \mathfrak{A} based on DCP. 1) Select the 0.1 percent brightest dark-channel pixels. 2) The most intense of these pixels in the original input image \mathfrak{I} is chosen to represent the atmospheric light.

2.2.2. Transmission Map

He et al. used a double min operation shown in (1) across all three-color channels to estimate the transmission map of a hazy image, as described in [23]:

$$\text{Min}_{y \in \mathcal{C}(x)} \left(\text{Min}_c \frac{I^c(y)}{\mathfrak{A}^c} \right) = \xi(x) \text{Min}_{y \in \mathcal{C}(x)} \left(\text{Min}_c \frac{\mathfrak{J}^c(y)}{\mathfrak{A}^c} \right) + 1 - \xi(x) \quad (3)$$

where $\xi(x)$ is the transmission map estimated, $I^c(y)$, $\mathfrak{J}^c(y)$, \mathfrak{A}^c are the c -th color component of input hazy image, dehazed image and atmospheric light, respectively. Since \mathfrak{A}^c is a positive constant, may derive (7) from (4):

$$\text{Min}_{y \in \mathcal{C}(x)} \left(\text{Min}_c \frac{\mathfrak{J}^c(y)}{\mathfrak{A}^c} \right) = 0 \quad (4)$$

getting (8) by substituting (7) for (5).

$$\tilde{t}(x) = 1 - \text{Min}_{y \in C(x)} \left(\text{Min}_c \frac{I^c(y)}{A^c} \right) \quad (5)$$

A predefined parameter ω ($0 < \omega \leq 1$) is initiated to evaluate the depth of the image; otherwise, the image will look artificial. This technique is known as 'aerial perspective' [24].

$$\tilde{t}(x) = 1 - \omega \text{Min}_{y \in C(x)} \left(\text{Min}_c \frac{I^c(y)}{A^c} \right) \quad (6)$$

2.3. Proposed Algorithm based on Intensity Feature

The observation reveals that the tissue of the pulmonary lesion in the CT radiomics images of lungs bears similarity to the hazy area. The depth-like map exhibits a distinct intensity that accurately captures the presence of haze. To generate the final haze corresponding to different positions, the principles of 2-DCP are employed to extract the intensity component from the depth-like map:

1. The Dark Channel Prior estimates the thickness of the tissue in the pulmonary lung lesion by selecting and extracting pixels within a specified threshold range (obtained through dataset analysis). This leads to the following equation:

$$\check{T}(x) = 1 - \tilde{t}(x) \quad (7)$$

And analysis condition:

$$\left((\check{T}(x) > 0.35) \ \&\& \ (\check{T}(x) < 0.70) \right) \quad (8)$$

where $\tilde{t}(x)$ is the transmission map estimated, $\check{T}(x)$ is the thickness contains pulmonary lesion intensity in input chest CT image.

1. The input chest CT image is auto segmented by reversing the DCP process to remove haze from pixels after estimation. However, when estimating pixels with haze in the chest pulmonary lesion, an IROI (Interest Region of Interest) is delineated by increasing the brightness of pixels within the specified threshold range during analysis. Alternatively, the original scene's radiance can be restored. As a result, the model can be represented by the following:

$$\check{T}(x) = \check{T}(x)_{\text{Brightness}} \quad (9)$$

Where, $\check{T}(x)_{\text{Brightness}}$ is the thickness contained pulmonary lesion intensity from brightness image.

2.4. Classifier: Resnet-50

Convolutional Neural Networks (CNNs) have recently demonstrated remarkable results in object recognition and classification tasks. Consequently, deep models based on convolutional neural networks (DNNs) have been developed by leveraging existing datasets. Rather than starting from scratch and training a model [25]. The proposed classifier chose the Resnet-50 architecture, which consists of 50 layers. An improvement was achieved by enhancing the brightness of the Region of Interest (ROI). This approach provides several advantages over classic algorithms and current state-of-the-art techniques, including Accelerated learning and better generalization effectiveness.

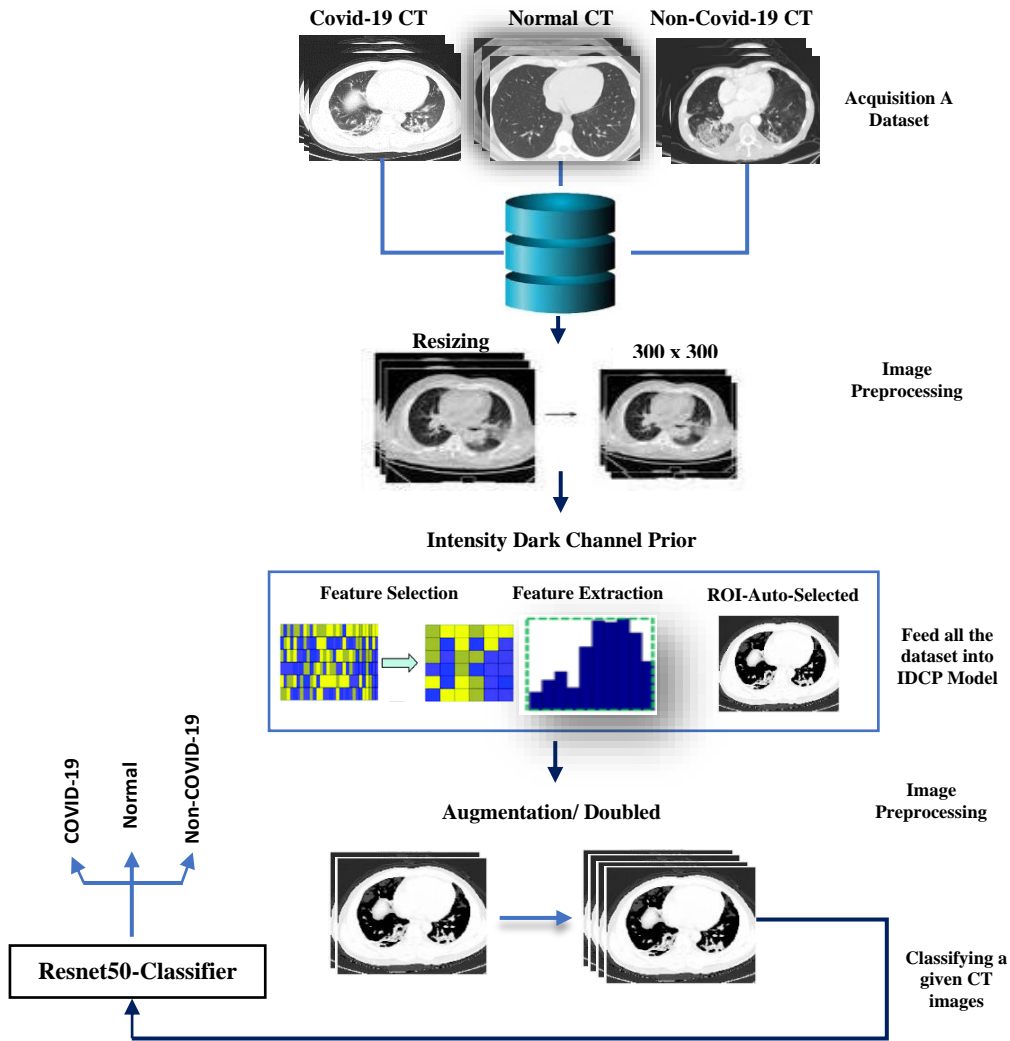


Figure 1. Architecture of the proposed ALS-IDCP-DNN model.

3. Experimental Results

The proposed model, Auto Lesion Segmentation-Intensity Dark Channel Prior, and Deep Neural Network (ALS-IDCP-DNN) were implemented using MATLAB software. For the experimental parts, a computer equipped with an Intel Xeon Silver 2.6 GHz processor, 16 GB RAM, and an NVIDIA GTX960M Quadro CPU card was used. The model was trained on CT radiomics scans for the classification of COVID-19 disease using the ResNet-50 framework that had been previously trained. Figure 2 presents the identification rates of COVID-19 disease in CT radiomics scans using the ALS-IDCP-DNN model, both with and without IDCP. The COVID-19 infected lesion is not only detected but also has its boundaries clearly visible, and its brightness is increased (indicated by the arrow). The outcomes demonstrated that incorporating DCP (Dark Channel Prior) and employing data augmentation approaches significantly enhanced individual performances. The performance measurements achieved remarkable rates, including 98.8% accuracy, 99% precision, 98% recall, and 98% F1-score. The method demonstrates a better accuracy of 98.8%. Out of 500 COVID-19 images, 500 non-COVID-19 images, and 500 healthy images, they were classified into their respective classes. Only 4 of the non-COVID-19 images were misclassified, resulting in a precision of 99%. Furthermore, out of the total non-COVID-19 images, only 2 were misclassified. A literature survey, presented in Table 1, compared the proposed method with recent studies that utilized the same dataset. While no significant tests were conducted in all the references, our method yielded significant results.

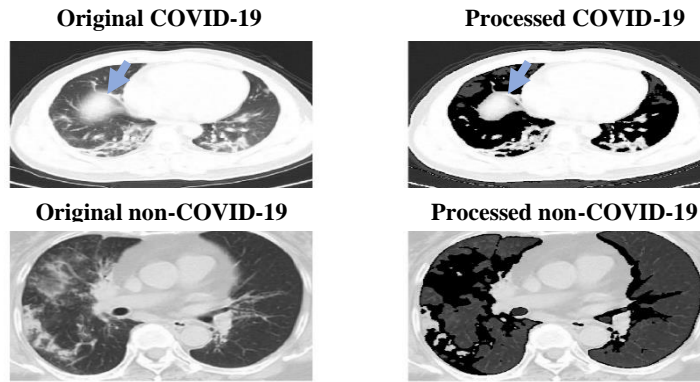


Figure 2. Samples with and without IDCP model.

Table 1. Assessment of the COVID-19 detection system in comparison to the latest studies.

No.	Author [ref]/Year	Methods	Accuracy	Sensitivity	Specificity	Epochs
1	de Sousa et al. [15]/ 2021	Ensemble	83%	NA	NA	200
2	Loey et al. [16] /2020	Resnet-50	82.91%	77.66%	87.62%	50
3	Saqib et. al. [17]/2020	DenseNet169	87%	NA	NA	500
4	Mishra et. al. [18] /2020	Deep CNN	88.34%	88.13%	90.5%	NL
5	Turkoglu et al. [26] /2021	MKs-ELM-DNN	98.4%	98.28%	98.44%	NL
6	Proposed Study/2022	DNN- without ALS-IDCP	86.61%	80.7%	90.6%	5
7	Proposed Study/2022	ALS-IDCP-DNN	98.8%	98%	99%	5

4. Conclusion

A new computer-aided system, known as the ALS-IDCP-DNN model, has been designed to enable swift diagnosis and prognosis of CT scan samples within the shortest possible time frame, utilizing only 5 epochs. To detect COVID-19, this study relied on a ResNet-50 model that had been previously trained. To address clustering difficulties and enhance the CT dataset, common data augmentation methods such as doubling and resizing were employed. The ALS-IDCP-DNN system combines the intensity dark channel prior scenario for enhanced auto-segmentation, feature selection, and extraction with deep transfer learning using the Resnet-50 model. According to this combination of metrics, including F1-score, accuracy, precision, and recall, the identification of COVID-19, non-COVID-19, and healthy CT scans achieved above 98%. Several pneumonia chest CT datasets have demonstrated that combining ResNet-50 with intensity segmentation and augmentation yields the most effective deep-learning algorithm for detecting COVID-19. Our model surpasses over 10 of the most advanced and effective methods currently available in diagnosing suspected COVID-19 patients, as evidenced by its superior ability to classify COVID-19 images. In the future, to differentiate between COVID-19 and other pulmonary conditions, we plan to incorporate automatic detection and segmentation.

5. Data Availability

<https://github.com/UCSD-AI4H/COVID-CT>.

References

- [1] <https://www.who.int/emergencies/diseases/novel-coronavirus-2019>
- [2] Xie X, Zhong Z, Zhao W, Zheng C, Wang F and Liu J 2020 Chest CT for Typical 2019-nCoV Pneumonia: Relationship to Negative RT-PCR Testing Radiology 296 E41–E45
- [3] Tao A, Zhenlu Y, Hongyan H, Chenao Z, Chong Ch, Wenzhi L, Qian T, Ziyong S and Liming X 2020 Correlation of Chest CT and RT-PCR Testing for Coronavirus Disease 2019 (COVID-19) in China: A Report of 1014 Cases Radiology 296 E32–E40
- [4] Martina P, Stefano C, Livia M, Emanuele M, Maurizio D, Nicola G, Maria R, Marco F, Carlo C and Valeria P 2021 Cross-sectional analysis of follow-up chest MRI and chest CT scans in patients previously affected by COVID-19 La radiologia medica 126 1273–1281
- [5] Nanshan Ch, Min Z, Xuan D, Jieming Q, Fengyun G, Yang H, Yang Q, Jingli W, Ying L, Yuan

- W, Jia'an X, Ting Y, Xinxin Z and Li Z 2020 Epidemiological and clinical characteristics of 99 cases of 2019 novel coronavirus pneumonia in Wuhan, China: a descriptive study *The Lancet* 395 507–513
- [6] Qian Y P, Xiao T W and Li N Z 2020 Findings of lung ultrasonography of novel corona virus pneumonia during the 2019–2020 epidemic *Intensive Care Med.* 46 849–850
- [7] Wuzhu L, Shushan Z, Binghui Ch, Jiabin Ch, Jianzhong X, Yuhong L, Hong Sh and Zhong Z S 2020 A Clinical Study of Noninvasive Assessment of Lung Lesions in Patients with Coronavirus Disease-19 (COVID-19) by Bedside Ultrasound *Ultraschall Med.* 41, 300–307
- [8] Soccorsa S, Andrea B, Marco M, Michele S, Damiano D, Giulio C, Esterita A, Francesco C and Cosima S 2020 Thoracic ultrasound and SARS-COVID-19: a pictorial essay *J. Ultrasound* 23 217
- [9] Hani C, Trieu N H, Saab I, Dangeard S, Bennani S, Chassagnon G and Revel M P 2020 COVID-19 pneumonia: A review of typical CT findings and differential diagnosis *Diagn. Interv. Imaging* 101 263–268
- [10] Ai T, et al. 2020 Correlation of Chest CT and RT-PCR Testing for Coronavirus Disease 2019 (COVID-19) in China: A Report of 1014 Cases *Radiology*, 296, E32–E40
- [11] Fang Y, et al. 2020 Sensitivity of Chest CT for COVID-19: Comparison to RT-PCR *Radiology*, 296, E115–E117
- [12] Caruso D, et al. 2020 Chest CT Features of COVID-19 in Rome, Italy *Radiology*, 296, E79–E85
- [13] Shuai W, Bo K, Jinlu M, Xianjun Z, Mingming X, Jia G, Mengjiao C, Jingyi Y, Yaodong L, Xiangfei M and Bo X 2021 A deep learning algorithm using CT images to screen for Corona virus disease (COVID-19) *Eur. Radiol.* 31 6096–6104
- [14] Tokodi M, Kovács A and Maurovich H P 2021 Radiomics in cardiovascular imaging: principles and clinical implications *Machine Learning in Cardiovascular Medicine* 31 281–310
- [15] De Sousa I P, Vellasco M and da Silva E C 2021 Explainable Artificial Intelligence for Bias Detection in COVID CT-Scan Classifiers *Sensors* 21 5657
- [16] Loey M, Manogaran G and Khalifa N E M 2020 A deep transfer learning model with classical data augmentation and CGAN to detect COVID-19 from chest CT radiography digital images. *Neural Comput. Appl.* 1–13
- [17] Saqib M, Anwar S, Anwar A, Petersson L, Sharma N and Blumenstein M 2022 COVID-19 Detection from Radiographs: Is Deep Learning Able to Handle the Crisis? *Sig.* 3 296-312
- [18] Arnab K M, Sujit K D, Pinki R and Sivaji B 2020 Identifying COVID19 from Chest CT Images: A Deep Convolutional Neural Networks Based Approach *J. Healthc Eng.* 2020 1-7
- [19] Aswathy A L, Anand H S and Vinod V C 2021 COVID-19 diagnosis and severity detection from CT-images using transfer learning and back propagation neural network *J. Infect. Public Health* 14 1435–1445
- [20] Kersting K 2018 Machine Learning and Artificial Intelligence: Two Fellow Travelers on the Quest for Intelligent Behavior in Machines *Front Big Data* 1 1-4
- [21] Nazari M, Shiri I and Zaidi H 2021 Radiomics-based machine learning model to predict risk of death within 5-years in clear cell renal cell carcinoma patients *Comput. Biol. Med.* 129 104135
- [22] Yang X, He X, Zhao J, Zhang Y, Zhang S and Xie P 2020 COVID-CT-Dataset: A CT Scan Dataset about COVID-19 arxiv.org/abs/2003.13865
- [23] He K, Sun J and Tang X 2011 Single image haze removal using dark channel prior *IEEE Trans. Pattern Anal. Mach. Intell.* 33 2341–2353
- [24] Peng Y T, Lu Z, Cheng F C, Zheng Y and Huang S C 2020 Image Haze Removal Using Airlight White Correction, Local Light Filter, and Aerial Perspective Prior *IEEE Transactions on Circuits and Systems for Video Technology* 30 1385–1395
- [25] He K, Zhang X, Ren S and Sun J 2016 Deep Residual Learning for Image Recognition *IEEE Computer Society Conf. on Computer Vision and Pattern Recognition* 770–778
- [26] Turkoglu M 2021 COVID-19 Detection System Using Chest CT Images and Multiple Kernels-Extreme Learning Machine Based on Deep Neural Network *IRBM* 42 207–214